Apoptosis (2016) 21:917–927
DOI 10.1007/s10495-016-1257-y

The antineoplastic agent α-bisabolol promotes cell death by inducing pores in mitochondria and lysosomes

Antonella Rigo[1] · **Fabrizio Vinante**[1]

Published online: 8 June 2016

Abstract The sesquiterpene α-bisabolol (α-BSB) has been shown to be an effective cytotoxic agent for a variety of human cancer cells in culture and animal models. However, much of its intracellular action remains elusive. We evaluated the cytotoxic action of α-BSB against CML-T1, Jurkat and HeLa cell lines, as preclinical models for myeloid, lymphoid and epithelial neoplasias. The approach included single cell analysis (flow cytometry, immunocytology) combined with cytotoxicity and proliferation assays to characterize organelle damage, autophagy, cytostatic effect, and apoptosis. The study focuses on the relevant steps in the cytotoxic cascade triggered by α-BSB: (1) the lipid rafts through which α-BSB enters the cells, (2) the opening of pores in the mitochondria and lysosomes, (3) the activation of both caspase-dependent and caspase-independent cell death pathways, (4) the induction of autophagy and (5) apoptosis. The effectiveness of α-BSB as an agent against tumor cells is grounded on its capability to act on different layers of cell regulation to elicit different concurrent death signals, thereby neutralizing a variety of aberrant survival mechanisms leading to treatment resistance in neoplastic cell.

Keywords α-bisabolol · Apoptosis · Autophagy · Lysosomes · Mitochondria · Neoplastic cell lines · BCL-2

✉ Fabrizio Vinante
fabrizio.vinante@univr.it

Antonella Rigo
antonella.rigo@univr.it

[1] Section of Hematology, Cancer Research & Cell Biology Laboratory, Department of Medicine, University of Verona, Verona, Italy

Abbreviations

AAF	Autophagic activity factor
AO	Acridine orange, a red fluorescent lysosomotropic probe
α-BSB	α-bisabolol
AM	Acetoxymethyl
CFSE	Carboxyfluorescein succinimidyl ester
CM	Complete medium
CM-H_2DCFDA	5-(and-6)-chloromethyl-2′,7′-dichlorodihydrofluorescein diacetate, acetyl ester
CML-T1, Jurkat, HeLa cell lines	Blast crisis of chronic myeloid leukemia, acute T cell leukemia, cervical cancer cell line, respectively
Cyto-ID® Green	Cationic amphiphilic tracer that selectively stains autophagic vacuoles
DAPI	4′,6-Diamidino-2-phenylindole, fluorescent nuclear counterstain
$\Delta\Psi_m$	Mitochondrial transmembrane potential
FSC	Forward scatter (in flow cytometry)
HBSS	Hank's balanced salt solution
IC_{50}	Half maximal inhibitory concentration
JC-1	5,5′,6,6′-Tetrachloro-1,1′,3,3′-tetraethylbenzimidazolylcarbocyanine iodide, red fluorescent mitochondrial counterstain
LT Green	Lysosomotropic probe
mPTP	Mitochondrial permeability transition pore
MTT	3-(4,5-Dimethylthiazol-2-yl)-2,5-diphenyltetrazolium bromide
Q-VD-Oph	Pan-caspase inhibitor
ROS	Reactive oxygen species
SSC	Side scatter (in flow cytometry)

TO-PRO®-3	Red-fluorescent nuclear and chromosome counterstain

Introduction

The plant-derived sesquiterpene alcohol α-bisabolol (α-BSB) has been found to be cytotoxic against a variety of human and animal neoplastic cells, ranging from leukemia [1–3] to pancreatic [4] and mammary [5] cancer cells to various cancer cell lines [6–9], at dosages devoid of organ toxicity in animal models [4, 5].

To date only partial descriptions of the mechanisms of action of α-BSB are available [1, 7–9]. The experimental evidence points to a pleiotropic effect targeting an array of cell structures and activities, including autophagy and apoptosis, which are typically crossregulated through BCL-2 family and autophagy gene-encoded molecules [10–21].

Sesquiterpenes like artemisinin [22] gossypol [23] or α-BSB that target these processes have theoretical and practical interest in fields ranging from neoplastic to infectious to inflammatory diseases. They are agents expected to have a killing potential against cells characterized by complex and multiple mechanisms of treatment resistance such as those encompassing tissue-derivation [4, 5], differentiation degree [1], proliferative kinetic and autocrine/paracrine loops [24–27] as well as defective apoptotic pathways [3, 5, 28–30] or constitutively activated autophagic mechanisms [2, 28, 29]. For instance, hematopoietic stem/progenitor cells make full use of autophagy [31, 32] and, not surprisingly, leukemic stem/progenitor cells are as likely to have autophagy programs activated as inhibited. In the end, autophagy can allow leukemic cells to escape otherwise effective treatment [33]. Nevertheless, we have found leukemic stem/progenitor cells to be sensitive to α-BSB [2, 29, 32].

We show here by using three well established preclinical models of highly undifferentiated myeloid, lymphoid and epithelial neoplasias, i.e. CML-T1, Jurkat and HeLa cell lines, respectively, that α-BSB enters cells through lipid rafts [2, 3, 6, 7, 9] and is able to induce membrane pores in both mitochondria and lysosomes, activating caspase-dependent [1–3, 8] or -independent death pathways and triggering both autophagy and apoptosis [10–21].

Materials and methods

Cells

CML-T1, Jurkat and HeLa cell lines (blast crisis of chronic myeloid leukemia, acute T cell leukemia and cervical cancer respectively) were purchased from DSMZ (Braunschweig, DE). Cells were cultured in RPMI-1640 (Invitrogen, Carlsbad, CA), supplemented with 10 % heat-inactivated fetal bovine serum (Invitrogen), 50 U/mL penicillin and 50 μg/mL streptomycin (complete medium, CM) and maintained at 37 °C in 5 % CO_2 [34].

Treatment with α-BSB

(−)-α-BSB at a purity ≥95 % (Sigma-Aldrich, St. Louis, MO) was dissolved in DMSO and a 500 μM stock solution in CM was prepared. The concentrations of α-BSB indicated in the different assays represent the calculated soluble fraction as reported elsewhere [1, 2].

Flow cytometry

Flow cytometry data were generated, acquired and analyzed by FACSCalibur cytometer (Becton Dickinson, San Jose, CA) and FlowJo 9.3.3 software (Tree Star, Ashland, OR).

Cell viability assay

Cells resuspended in CM, seeded at a density of 3×10^4 cells/mL in 96-well plates and incubated at 37 °C in 5 % CO_2 were exposed to 10, 20, 40, 80, 160 μM α-BSB for up to 96 h. In selected experiments 25 μM caspase inhibitor Q-VD-OPh (Calbiochem, Billerica, MA) [35] was added to Jurkat cells 30 min before α-BSB treatment. At the end of the culture, viability was measured by 3-(4, 5-dimethylthiazol-2-yl)-2,5-diphenyltetrazolium bromide (MTT, Sigma-Aldrich) incorporation as previously described [36]. Viability was expressed as the ratio between the number of cells treated with α-BSB and the number of cells treated with the vehicle alone.

α-BSB uptake assay

Cells were resuspended in CM, seeded at a density of 3×10^4 cells/mL in 96-well plates in the absence or presence of 1–1.5 μg/mL Filipin III (Sigma-Aldrich) and incubated 90 min at 37 °C in 5 % CO_2. Then they were exposed for 24 h to 20, 40, 80 μM α-BSB and viability was measured by MTT incorporation as reported above. Data were expressed as percentage of rescue from apoptosis in Filipin III treated cells as compared to untreated ones.

Proliferation assay

24-h-starved cells were labeled with CFSE (Invitrogen), as described previously [37]. Briefly, cells were resuspended at a final concentration of 10^7 cells/mL in PBS/5 % FCS.

CFSE was added at a final concentration of 5 μM and incubated for 5 min at room temperature. The reaction was stopped by washing twice with PBS/5 % FCS. Cells were plated at 10^6 cells/mL in CM and exposed to 10, 20, 40, 80, 160 μM of α-BSB. Every 24 h for 4 days an aliquot of cells was harvested, added with TO-PRO-3 (Invitrogen) and subjected to flow cytometry.

Apoptosis assay

Cell lines were treated for 1–96 h with 20–80 μM α-BSB, then washed with PBS and stained with Annexin-V-FITC (Miltenyi Biotec, Bergisch Gladbach, DE) for 15 min following manufacturer's instructions. TO-PRO-3 was added immediately before acquisition by flow cytometry (FL-1 and FL-4 channels). In selected experiments Jurkat cells were preincubated for 4 h with the autophagy inhibitors 3-methyladenine (3-MA, 5 mM, Sigma-Aldrich) and bafilomycin A (BafA 100 nM, Sigma-Aldrich). Then they were stimulated with 20 and 40 μM α-BSB for 24 h and viability was measured by MTT and AnnexinV-FITC/TO-PRO-3 assays. If needed, necrosis was differentiated as cell swelling and plasma membrane breakdown by using phase contrast optics.

Autophagy assay

Cells were resuspended in CM and exposed for 1–96 h to 20, 40 and 80 μM α-BSB. Then they were washed in PBS and stained (Cyto-ID Autophagy Detection Kit, Enzo Life Science, Farmingdale, NY). Cellular fluorescence was evaluated on Fl-1 channel. Cells incubated 2 h in HBSS without serum (starvation) were used as positive control of autophagy. Data were expressed as autophagic activity factor: $AAF = 100 \times (MFI_{treated} - MFI_{control})/MFI_{treated}$ where MFI is the median fluorescence intensity of the cells.

Detection of intracellular reactive oxygen species (ROS)

Cells were incubated with 40 or 80 μM α-BSB for 2 h, then washed, resuspended in HBSS (Invitrogen) at 5×10^5/mL and loaded with 2.5 μM of CM-H_2DCFDA (Molecular Probes) for 1 h at 37 °C. After washing, ROS were evaluated in flow cytometry by measuring the green fluorescence signal of DCF, the oxidation product of CM-H_2DCFDA by free radicals. H_2O_2 was used as positive control.

Mitochondrial injury assays

Cells were resuspended in CM at 1×10^6/mL and treated with 40 μM α-BSB for 3 and 5 h at 37 °C. (1) *Mitochondrial permeability transition pore (mPTP) opening*. Cells were washed with CM, resuspended with HBSS/Ca^{2+} and loaded with 10 nM calcein AM with or without 400 μM $CoCl_2$ for 15 min at 37 °C (MitoProbe Transition Pore Assay Kit, Invitrogen). Cell fluorescence was recorded by flow cytometry. (2) *Mitochondrial transmembrane potential* ($\Delta\Psi_m$). As previously described [1], cells were washed with prewarmed CM, loaded with 4 μM JC-1 (Molecular Probes, Eugene, OR) [38, 39] and after 30 min incubation they were washed twice with PBS. An aliquot of each sample was resuspended in PBS and analyzed by flow cytometry. The remaining aliquot of each sample was spotted onto a slide, immobilized under a coverslip and immediately recorded by an Axio Observer inverted microscope (Zeiss, Gottingen, DE). Visualization of JC-1 monomers (green fluorescence) and JC-1 aggregates (red fluorescence) was done using filter sets for fluorescein and rhodamine dyes. Image analysis was done by Axiovision 3 software.

Lysosome injury assays

(1) *Acridine orange (AO)-uptake assay*. Cells treated with 80 μM α-BSB for 1 and 3 h were stained with 0.5 μg/mL AO for 15 min at 37 °C, washed twice and acquired by flow cytometry (FL-3 channel). (2) *AO-relocation assay*. Cells incubated with 0.5 μg/mL AO (Molecular Probes) for 15 min at 37 °C, washed twice with RPMI-1640 and incubated with 40, 60, 80 μM α-BSB for 1 and 3 h, were acquired by flow cytometry (FL-1 channel). (3) *LysoTracker green (LTG)-uptake assay*. Cells treated with 80 μM α-BSB for 1, 3 and 5 h were washed and incubated at 37 °C for 1 h with 75 nM of the acidotropic dye LTG DND-26 (LTG, Molecular Probes). Cells were acquired by flow cytometry (FL-1 channel) or counterstained with Hoechst 33342 (Invitrogen), transferred to a slide and imaged by an Axio Observer inverted microscope. (4) *Cathepsin B immunofluorescence staining*. Hela cells were grown on slides until semiconfluence, exposed to 80 μM α-BSB for 1, 3 and 5 h, washed in PBS and fixed in methanol at −20 °C for 20 min. After a brief rinsing in cold acetone cells were blocked for 1 h in PBS/5 % normal goat serum and incubated overnight at 4 °C with a rabbit monoclonal antibody to human cathepsin B (Abcam, Cambridge, UK) in PBS/0.1 % Triton X-100. The cell samples were developed with a goat anti-rabbit Alexa Fluor 568-conjugated antibody (Invitrogen), counterstained with DAPI and imaged by an Axio Observer inverted microscope.

Statistics

Student's t test for means, χ^2 tests and Kruskall–Wallis analysis of variance by rank as appropriate were considered significant for p values <0.05.

Results

Cytotoxicity

Exposure to α-BSB reduced cell viability in a dose-dependent manner. In the experiments depicted in Fig. 1a, α-BSB IC_{50} was 52 ± 7, 80 ± 3 and 95 ± 9 μM in CML-T1, Jurkat and HeLa cells, respectively. The different IC_{50} may reflect either characteristics of the different cell lineages or differential patterns of tumor-related mutations or metabolism. The loss of cell viability was associated with several activities enacted by α-BSB. (1) *Apoptosis*. In the experiment in Fig. 1b, α-BSB induced a time-dependent increase of Annexin-V and TO-PRO-3 fluorescence, indicating the activation of the apoptotic cascade. (2) *Caspase-independent death*. Figure 1c shows that treatment with the broad spectrum caspase inhibitor Q-VD-OPh was only partially effective in blocking the apoptotic effects induced by α-BSB, suggesting that death pathways different from the apoptotic ones were activated and induced loss of cell viability [35]. (3) *Cytostatic effect*. In Fig. 1d, parallel experiments of cell proliferation are depicted, as evaluated by CSFE assay. α-BSB induced a lesser decrease of mean fluorescence intensity (MFI), i.e. longer S-phases, as opposed to untreated cells at each time, a feature in line with the activation of autophagic processes. In the following paragraphs we will analyze in detail such different α-BSB-induced activities.

Lipid raft-mediated internalization

It has been demonstrated that cell membrane lipid rafts are targets of α-BSB [9]. The exact role, however, if any, played by lipid rafts in the mechanism of α-BSB entry into cells remained an unsolved question. To characterize the relevance of lipid rafts in the process of α-BSB internalization, we disrupted them by pretreating cells with Filipin III. As shown in Fig. 2, Filipin III rescued cells from α-BSB cytotoxicity in a dose-dependent manner. Therefore, lipid raft-dependent endocytosis plays a role in α-BSB internalization that leads to cell toxicity.

Mitochondrial destabilization

We have previously demonstrated that treatment with α-BSB induced dissipation of the $\Delta\Psi_m$ in leukemic cell lines as well as in leukemic primary cells [1–3]. Here we analysed these events in CML-T1, Jurkat and HeLa cell lines. As shown in Fig. 2b, the cells were incubated with α-BSB and then loaded with calcein acetoxymethyl (AM) that becomes fluorescent in cytoplasm and mitochondria, and added with $CoCl_2$, a quenching compound that enters

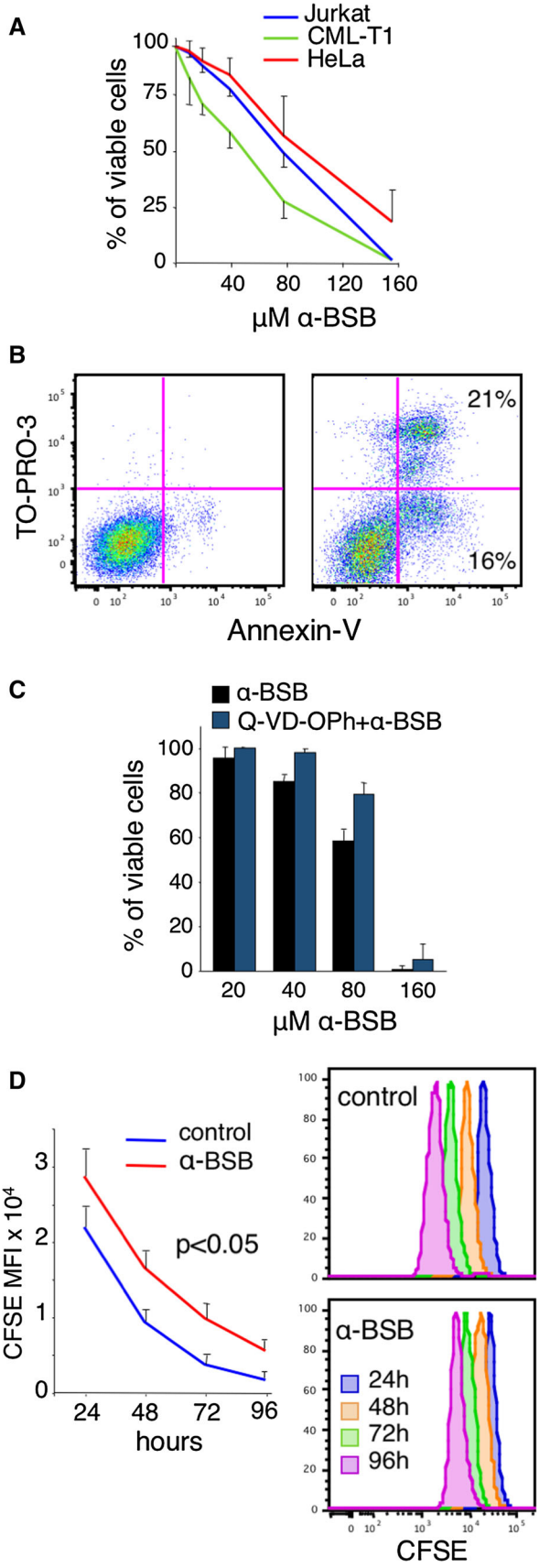

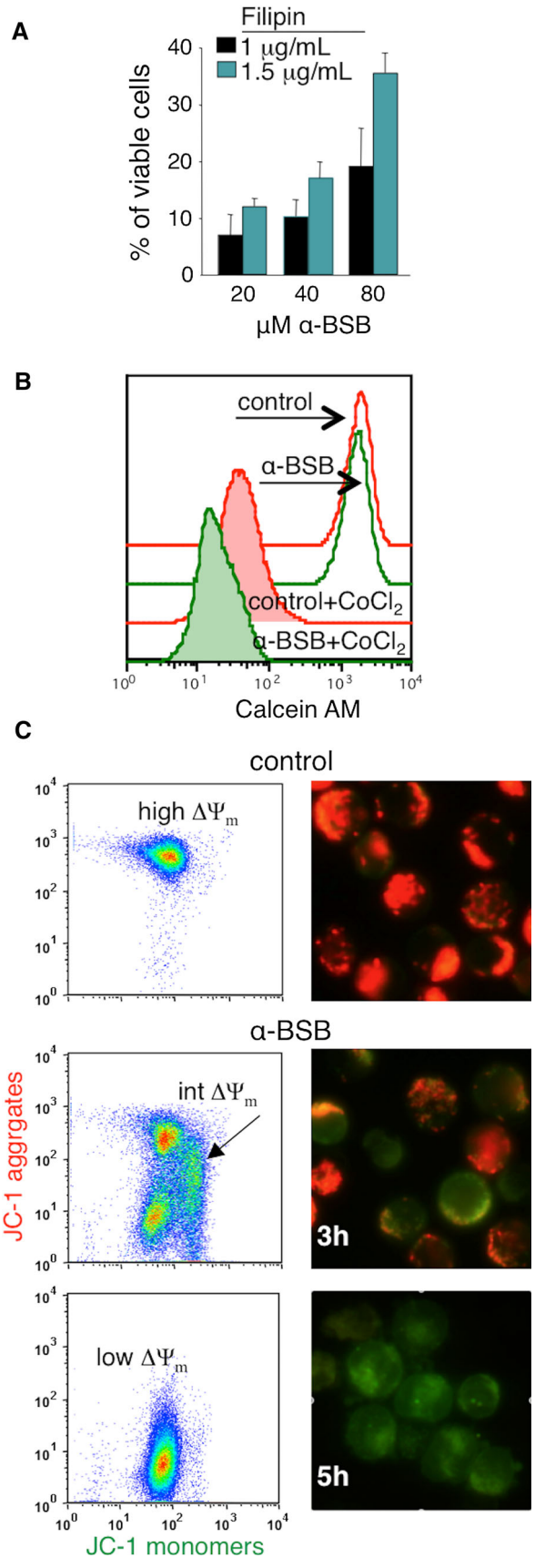

◀**Fig. 1** α-BSB activities on cell viability, apoptosis and proliferation. **a** Viability of cells treated with α-BSB for 48 h. **b** Apoptosis of cells treated with 80 μM α-BSB for 1 and 3 h. Staining with Annexin-V and TO-PRO-3 to distinguish between alive (Annexin-V^{neg}/TO-PRO-3^{neg}), early apoptotic (Annexin-V^{pos}/TO-PRO-3^{neg}), late apoptotic (Annexin-V^{pos}/TO-PRO-3^{pos}) and necrotic (Annexin-V^{neg}/TO-PRO-3^{pos}) cells. **c** Effects of 25 μM pancaspase inhibitor Q-VD-OPh on the viability of cells treated with α-BSB for 48 h. The inhibition of death was statistically significant ($p < 0.05$). **d** *Left side.* 96-h time-course comparison of the CFSE fluorescence intensity between control and treated cells (MFI ± SD, $p < 0.05$). *Right side.* Representative overlay histogram of the daily CFSE fluorescence intensity in alive cells (TO-PRO-3^{neg} population). In control cells, CFSE dilution amongst the proliferating cells induced a given decrease of fluorescence intensity day by day. In 40 μM α-BSB-treated cells a lesser dilution of CFSE indicated decreased cell division. Note that proliferating cell lines generated a single peak of CSFE characterized by a gradual decrease of MFI over time. Representative experiments or mean ± SD of at least five experiments are depicted

mitochondria only in the presence of pores in their membrane. A clear-cut decrease of the fluorescence emitted by treated cells as opposed to the untreated ones indicated mitochondrial pore opening. Then cells were stained with JC-1, a fluorescence emitter preferentially driven by the $\Delta\Psi_m$ to mitochondria, where it forms red-emitting aggregates, whereas in the cytosol it exists as a green-fluorescent monomer. The ratio of red/green JC-1 fluorescence is a reliable measure of $\Delta\Psi_m$ [40]. At flow cytometry, cells exposed to α-BSB lost their red fluorescence, shifting downward over a few hours (Fig. 2c, *left side*). At microscopy, treated cells changed from a punctate red to a diffuse green fluorescence to indicate disruption of $\Delta\Psi_m$ (Fig. 2c, *right side*). Taken together, the calcein AM/$CoCl_2$ and JC-1 assays show that α-BSB induces irreversible mPTP opening (Fig. 2b) with dissipation of the $\Delta\Psi_m$ (Fig. 2c). This is followed by cytochrome *c* release, the start of the caspase-dependent apoptotic process and the loss of cell viability (Fig. 1a, b). The evidence, however, that α-BSB induced cell death despite caspase blocking (Fig. 1c) led us to investigate other kinds of organelle damage beside the mitochondrial loss of $\Delta\Psi_m$.

Lysosomal membrane permeabilization

The effect of α-BSB on lysosomes was studied by using the lysosomotropic probes AO (red fluorescent) and LTG (green fluorescent), both of which are retained in intact lysosomes and emit intense fluorescence at flow cytometry. Damaged lysosomes release AO to the cytosol, which turns green [41, 42]. The AO-uptake assay measures directly the red lysosomal fluorescence. Instead, the AO-relocation assay is based on the assessment of increased cytosolic green fluorescence secondary to lysosomal rupture with AO relocation to the cytosol [42–45]. After treatment with

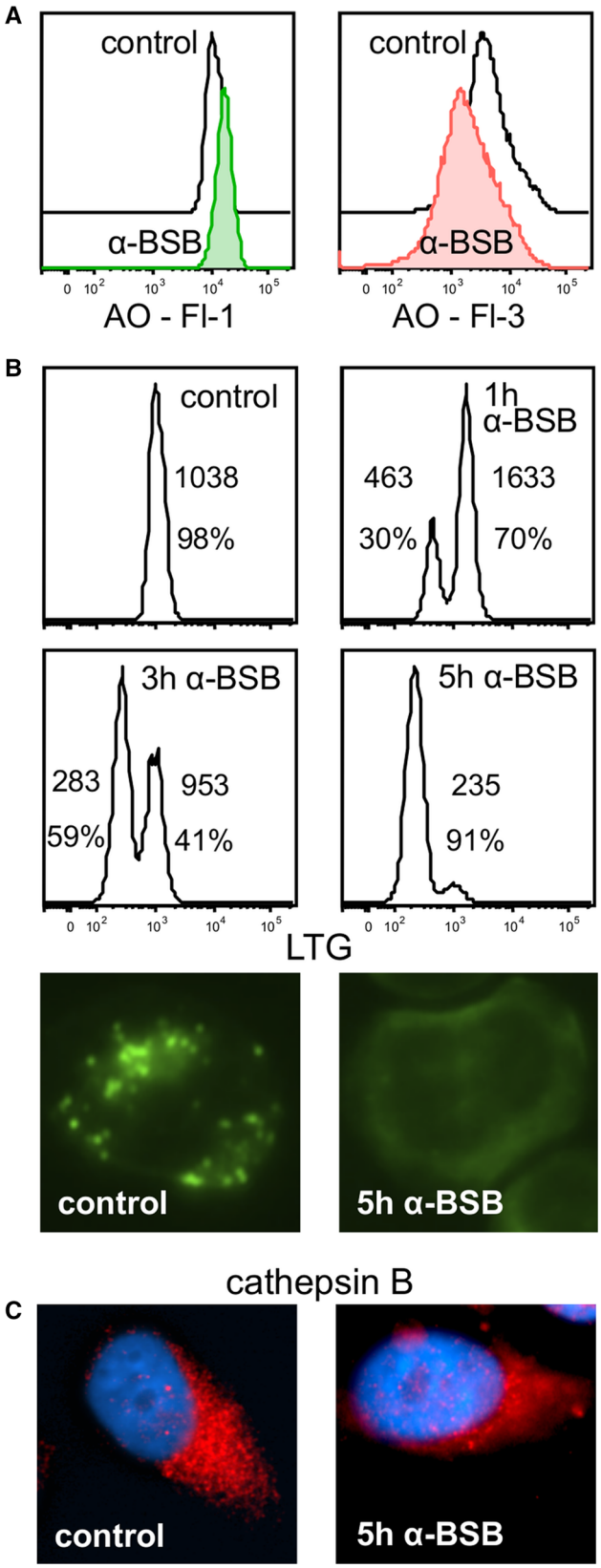

◀**Fig. 2** α-BSB enters cells via lipid rafts and induces mitochondrial membrane injury. **a** Pretreatment with 1 and 1.5 μg/mL Filipin III (which disrupt lipid rafts with no leakage through the membrane) rescued from apoptosis 7 ± 3.6, 10 ± 2.9, 19 ± 6.7 and 12 ± 1.4, 17 ± 2.8, 35 ± 3.5 %, respectively, of the cells exposed to 20, 40, 80 μM α-BSB for 24 h ($p < 0.05$). **b** α-BSB-induced mPTP opening. After 5 h of treatment with 40 μM α-BSB, cells loaded with calcein AM ester and added with $CoCl_2$ were significantly less fluorescent than untreated cells ($p < 0.01$), indicating the presence of pores in mitochondrial membrane allowing $CoCl_2$ to pass through. **c** α-BSB-induced dissipation of $\Delta\Psi_m$ is indicated by JC-1 relocation from mitochondria (red-fluorescent aggregates) to cytoplasm (green-fluorescent monomer). *Flow cytometry (left side)*. Untreated cells showed high red fluorescent JC-1 aggregates corresponding to normal (high) $\Delta\Psi_m$. Treatment with 40 μM α-BSB for 3 and 5 h induced progressive reduction of the red fluorescence, i.e. JC-1 relocation to the cytosol, due to the α-BSB-induced progressive loss of $\Delta\Psi_m$ (intermediate and low $\Delta\Psi_m$). *Fluorescence microscopy* (X400, *right side*). Untreated cells show intact, well-polarized mitochondria, marked by a *red punctate fluorescence*; after treatment with 40 μM α-BSB for 3 and 5 h, a *green fluorescence* indicates the relocation of JC-1 to cytosol (green-fluorescent monomers) due to loss of $\Delta\Psi_m$. Representative experiments or mean ± SD of at least five experiments are depicted

α-BSB, the AO-relocation assay demonstrated an increase in green fluorescence detectable up to 3 h (Fig. 3a, *left side*) and, accordingly, the AO-uptake assay demonstrated a decrease in red fluorescence (Fig. 3a, *right side*), both assays indicating the alteration of the lysosomal membrane permeability by α-BSB. This was further confirmed by the LTG-uptake assay [46, 47]. Under baseline conditions, LTG was located at large green fluorescent vesicles in the cytoplasm. It showed higher MFI within 1 h of treatment with α-BSB and a time-dependent appearance of an incremental population of dimly fluorescent cells (Fig. 3b, *top*). These flow cytometry findings are consistent with an enlargement and subsequent collapse of lysosomes due to α-BSB. At microscopy we could directly observe a shift from a speckled cytosolic pattern in untreated cells to a diffuse pale extralysosomal pattern after 5 h of treatment (Fig. 3b, *bottom*) in line with an alteration of the lysosomal membrane permeability. Immunofluorescence staining of cathepsin B confirmed the α-BSB-induced leakage of lysosomal contents into the cytosol. In untreated cells cathepsin B showed a cytoplasmic punctate pattern with a typical higher concentration in the perinuclear region (Fig. 3c, *left side*). Following exposure to α-BSB there was a clear leakage of cathepsin B out around lysosomes into the cytosol as demonstrated by diffuse cytoplasmic positivity (Fig. 3c, *right side*). Therefore α-BSB triggers irreversible opening in the lysosomal membrane (Fig. 3a–c) and may explain why the pan-caspase inhibitor Q-VD-OPh induced only a partial blockade of the α-BSB cytotoxicity (Fig. 1c).

◀**Fig. 3** α-BSB induces lysosomal membrane injury. Cells were incubated in the presence or absence of 40 μM α-BSB up to 5 h and stained with AO, LTG and immunofluorescence to lysosomal enzyme cathepsin B. **a** *Left side* AO-relocation assay shows an increase of green fluorescence by flow cytometry indicating a leakage of AO from lysosomes into the cytoplasm. *Right side* AO-uptake assay measures a reduction in red fluorescence due to defective lysosomal accumulation of AO. **b** *Flow cytometry.* Kinetics of lysosomal destabilization as evaluated by LTG-uptake assay showing initial enhancement of fluorescence followed by collapse (MFI values and the corresponding percentage of cells are reported). *Fluorescence microscopy* (X1000). Shift from a punctate staining (intact lysosomes) in control cells to a diffuse extralysosomal signal (lysosomal destabilization) in treated cells. (**c**) Immunostaining of cathepsin B (X1000 *fluorescence microscopy*). The *red punctate* distribution of the cathepsin preferentially in the perinuclear region of control cells is replaced by a diffuse cytosolic pattern throughout the cell after exposure to α-BSB. Nuclei counterstained with DAPI. Representative experiments out of five are depicted

ROS induction

The cell-permeant probe CM-H_2DCFDA is nonfluorescent until removal of the acetate groups by intracellular esterases. Therefore the intensity of CM-H_2DCFDA fluorescence is proportional to the cellular amount of ROS. In Jurkat cells treated with 40 and 80 μM α-BSB for 2 h (Fig. 4a) there was a clear increase of fluorescence of CM-H_2DCFDA loaded cells ($MFI_{treated} = 35 \pm 3$ vs $MFI_{basal} = 8.5 \pm 0.5$; $p < 0.01$), indicating ROS generation, which is associated with lysosome injury and mitochondrial disruption [21, 48].

Autophagy and apoptosis

Damaged cells are expected to undergo an attempt of rescue through autophagy and to undergo apoptosis if the rescue fails [11]. Therefore, the α-BSB-dependent cytostatic effect shown in Fig. 1d experiments could signal autophagy. To study this we first obtained FSC-A versus SSC-A cytograms of α-BSB-treated cells to roughly discriminate between living (G1) and apoptotic (G2) cells (Fig. 4b, *top*). G1 cells were still alive, while G2 cells were apoptotic, as shown in Fig. 4b, *bottom*. Then we used Cyto-ID-green, to measure autophagic vacuoles in live cells. The dye exhibits bright fluorescence upon incorporation into preautophagosomes, autophagosomes and autophagolysosomes. Analysis on the G1 population loaded with Cyto-ID-green evidenced a dose response increase of green fluorescence (Fig. 4c, *left side*): the autophagic activity factor raised up to 50.5 ± 10.4 upon increasing concentrations of α-BSB as opposed to 31.6 ± 7.5 in starved cells used as a control, which indicated active autophagy (Fig. 4c, *right side*). By contrast, analysis on the G2 population demonstrated a reduction of fluorescence, as a result of dye leakage (data not shown) in line with apoptosis. An increase of Cyto-ID-green-related fluorescence may signal either induction of autophagy or accumulation of autophagosomes following inhibition of the autophagic flux, namely due to damaged lysosomes. But autophagy takes place in both cases. The dose– and time– response experiments in Fig. 5 further supported this interpretation. The rescue effect of autophagy was measured as increased number of cells at each analysis-point as opposed to seeded cells. Up to 20 μM α-BSB, the autophagic rescue was efficient. At higher α-BSB concentrations and longer times cumulative lysosomal damage inhibited autophagy likely by impairing the autophagic flux. The highest α-BSB doses led to necrosis. This was supported by the experiments shown in Fig. 6, where the inhibition of autophagy by using 3-MA and BafA led to a clear-cut increase of apoptotic death in the range of 20–40 μM α-BSB.

Discussion

In the present work we investigated the mechanisms of cell death induced by the plant-derived sesquiterpene α-BSB. Our findings show that this agent promotes cytotoxicity by inducing pores in mitochondria and lysosomes. Loss of $\Delta\Psi_m$, lysosome leakage, and apoptosis follow. Autophagy activated first as a rescue response to α-BSB-induced damage is bound to fail due to lysosome permeabilization. Eventually, both mitochondrial and lysosomal damages cooperate in activating caspases and cell apoptosis.

Lysosomal variation may be a predisposing factor for disease [49] and some alterations have been described in malignancy that highlight the role of lysosomes both in cancer pathogenesis and treatment [21, 29]. Often cancer cells share overexpression of lysosomal proteases that promote cancer growth, invasion and metastasis or cells bear acquired defects in the classic caspase-dependent pathways of apoptosis that favor survival as well as resistance to agents acting through those pathways. Therefore, enhancing lysosomal cell-death pathways may be a therapeutic strategy to overcome those acquired defects [29].

On the other hand, lysosomes are involved in autophagy. This regulated mechanism sequesters parts of the cytoplasm and organelles and delivers them to lysosomes for degradation. Autophagy protects cells against starvation (recycling nutrient from digested organelles), ensures cell homeostasis (removing damaged protein and organelle), and is involved in aging, cancer and degenerative diseases [11, 12, 50]. Convincing data show that cancer stem cells may survive treatment due to autophagy [29, 31, 32]. For example, BCR/ABL + stem cells represent a leukemic reservoir that resists tyrosine kinase inhibitors through autophagy [1, 2]. α-BSB by damaging lysosomes and

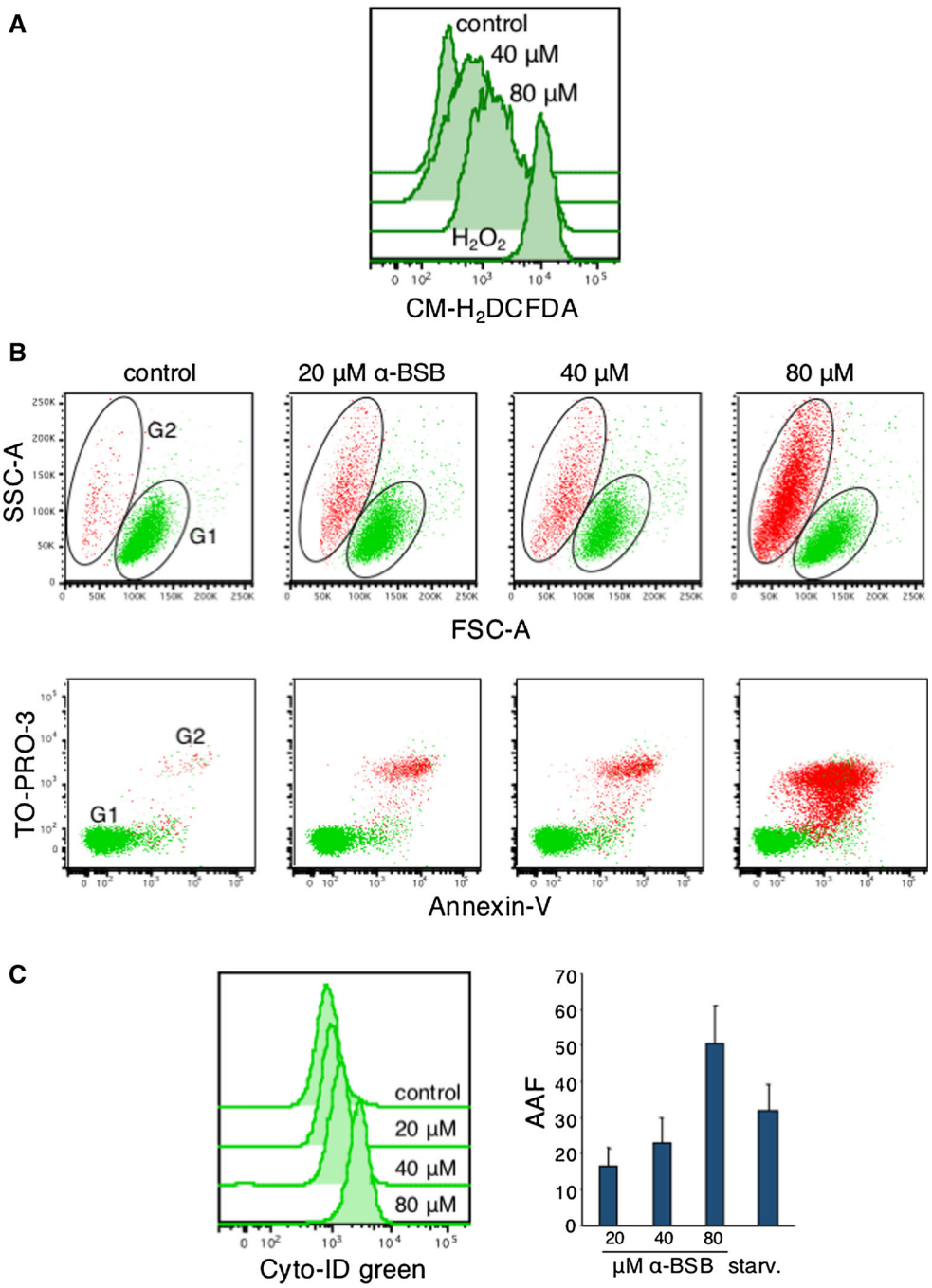

Fig. 4 α-BSB induces autophagy and apoptosis. Cells were cultured for 2 and 5 h in the presence of α-BSB at the indicated doses. Then each sample was divided in three aliquots to test ROS generation, autophagy and apoptosis. **a** Dose–response generation of ROS in Jurkat cells as evidenced by the increase of green fluorescence of CM-H_2DCFDA. Incubation with H_2O_2 was used as positive control. **b** *Top* FSC-A versus SSC-A cytograms. Gate 1 (G1) and gate 2 (G2) were applied to evidence alive and dead cells based on their morphological pattern. *Bottom* Analysis of apoptosis. G1, alive cells (Annexin V^{neg}/TO-PRO-3^{neg}); G2, apoptotic cells (Annexin V^{pos}/TO-PRO-3^{pos}). **c** *Left side* Dose–response increase of fluorescence in α-BSB-treated cells from G1 population stained with Cyto-ID-green autophagy detection tracer. *Right side* Upon α-BSB the AAF rose significantly even as compared to the positive control (cells starved in HBSS). Representative results or mean ± SD of at least five experiments are depicted

inhibiting the autophagic flux may contribute to target such cancer reservoirs whose survival depends on autophagic mechanisms [29, 31, 32]. Indeed, lysosomal permeabilization with the release of proteolytic enzymes is a recognized trigger for apoptosis and inhibition of autophagy [11, 21]. For example, TNF-related apoptosis-inducing ligand (TRAIL) induces apoptosis through lysosomal permeabilization supported by BCL-2-associated X protein (BAX), for BAX siRNA reduced cell death following stimulation with TRAIL [29]. TNFα-induced hepatocyte apoptosis is mediated through the BCL-2 homology 3 (BH3)-only protein BH3-interacting domain death agonist (BID) upstream of lysosome-dependent caspase 2 activation [51].

Accordingly, our working hypothesis is that the effects of α-BSB on mammal cells may involve the interaction of α-BSB and BID, which based on previous structural analysis harbors a pocket chemically recognized by α-BSB [9]. The switch from autophagy to apoptosis eventually induced by α-BSB in our experiments may be prevalently a

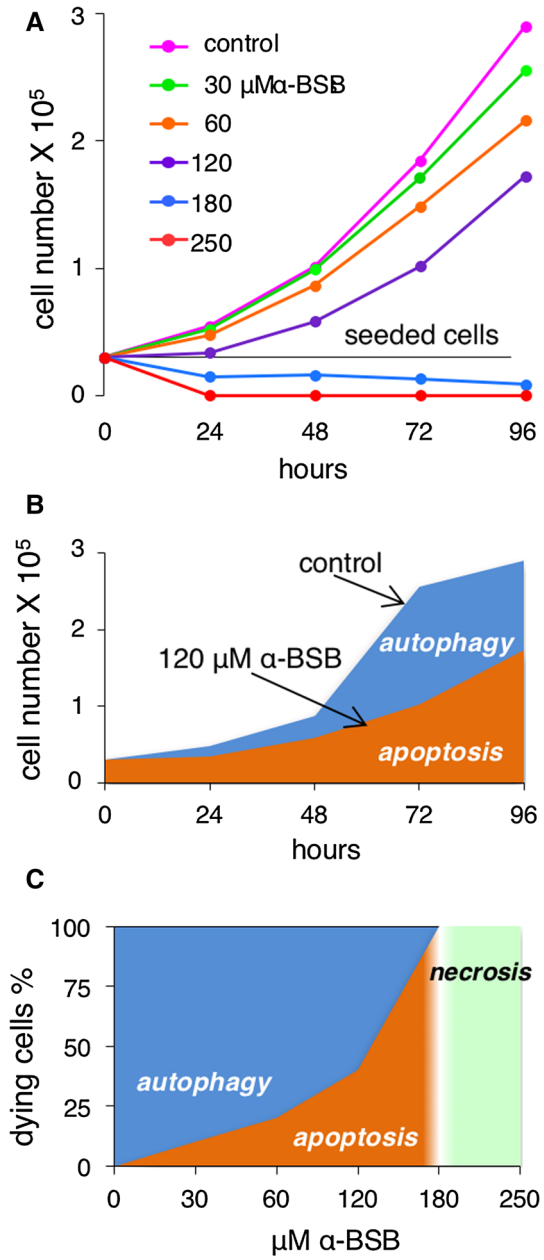

Fig. 5 Relationship between α-BSB-dependent autophagy, apoptosis and necrosis. Cell number was determined by MTT after α-BSB treatment at the indicated concentrations and times. **a** Absolute number of cells in untreated and α-BSB-treated samples. **b** Comparison of proliferation between untreated and 120 μM α-BSB-treated cells. **c** The dying-cell percentages related to the α-BSB concentrations suggested activation and then subversion of protective autophagy [11]. Apoptosis eventually prevailed, while the highest α-BSB doses induced necrosis, which was evaluated by phase contrast optics as cell swelling and plasma membrane breakdown. *Orange*, *blue* and *green areas* indicate apoptotic cell loss, autophagic cell rescue and necrosis, respectively. Mean ± SD of at least five experiments are depicted

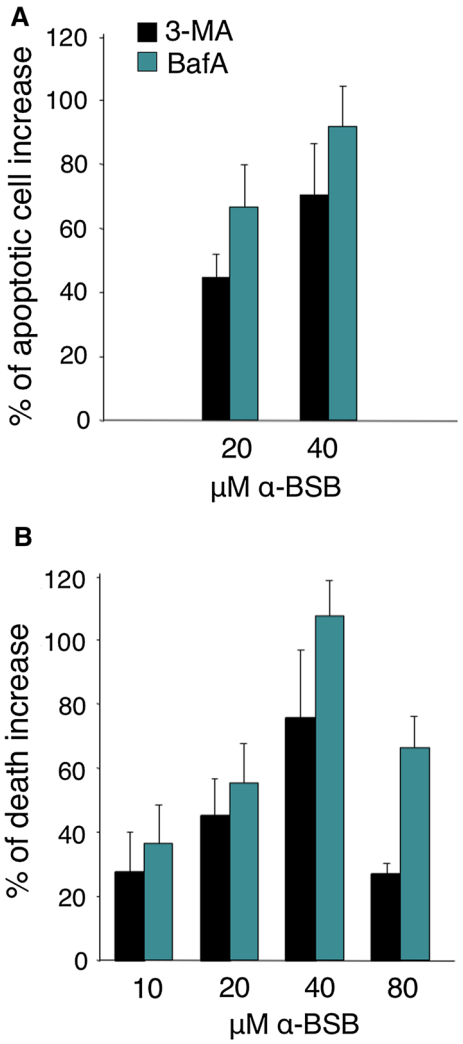

Fig. 6 Autophagy inhibitors increase α-BSB apoptotic activity. Jurkat cells were pretreated with BafA and 3-MA and then with the indicated doses of α-BSB for 24 h. **a** Viability measurement by AnnexinV-FITC/TO-PRO-3 assay. The percentages are reported of increase of apoptotic cells (i.e. $AnxV^{pos}/TO\text{-}PRO\text{-}3^{neg}$ + $AnxV^{pos}/TO\text{-}PRO\text{-}3^{pos}$) after α-BSB stimulation in cells pretreated with autophagy inhibitors as opposed to untreated ones ($p < 0.01$). **b** Viability measurement by MTT assay. Percentages of cellular death increase after α-BSB stimulation in cells pretreated with autophagy inhibitors as opposed to untreated ones ($p < 0.01$). Mean ± SD of four experiments are depicted

consequence of the lysosomal damage inhibiting autophagy and tipping the balance towards apoptosis [11, 14, 16–20, 52, 53]. Lower dosages of α-BSB activated autophagy, while higher dosages determined apoptosis or even necrosis. This is in line with the cytostatic effect (Fig. 1c, d), with the relationship between concentration/time and autophagy/apoptosis/necrosis (Figs. 4, 5) and with the increase of apoptosis induced by inhibiting autophagy (Fig. 6) that we could measure in our experiments following the treatment with α-BSB.

The specific effects of α-BSB, a terpene alcohol, on mammal cells may be achieved through a xenohormesis [54] layered over a pre-existing chemical foundation that comes

from ancient molecular interactions regulating apoptosis/autophagy switches shared by plant and mammal cells. In plant cell immunity, terpenes amongst other molecules act as pore-opening antimicrobial agents, apoptosis/autophagy regulators, mediators of hormone defense networking and eventually as cell fate regulator [13, 55–60], a context where autophagy may represent the oldest form of eukaryotic innate immunity to survive microorganisms.

In conclusion, α-BSB is a plant-derived agent effective in inducing cytotoxicity in preclinical cellular and animal models. Its activities in mammal cells are probably founded on a layer of ancient and basic molecular interactions conserved over evolutionary distances [55–62]. In the present study we showed that α-BSB kills neoplastic cells through cascade affects of mitochondria [7, 20] and lysosomes eventually subverting autophagic protective mechanisms and inducing apoptosis [11, 21]. For α-BSB may recruit either caspase-dependent or caspase-independent cell death pathways, it is a cytotoxic agent able to overcome various mechanisms of resistance to treatment that neoplastic cells have acquired.

Acknowledgments FV wants to express his gratitude to Maria Langhieri for supporting cancer research in memory of her mother Iliana Tescaroli.

Authors' contribution FV conceived the research. AR performed the experiments. Both authors contributed to concept design, analyzed data, discussed results, wrote and approved the final manuscript.

Funding This work was supported by funding from Italian Association for Cancer Research (AIRC, Milan, Italy)/Cariverona Foundation (Verona, Italy). The funders had no role in study design, data collection and analysis, decision to publish, or preparation of the manuscript.

Compliance with ethical standards

Conflict of interest The authors declare they have no competing interests.

References

1. Cavalieri E, Rigo A, Bonifacio M, Carcereri de Prati A, Guardalben E, Bergamini C et al (2011) Pro-apoptotic activity of α-bisabolol in preclinical models of primary human acute leukemia cells. J Transl Med 9:45–57
2. Bonifacio M, Rigo A, Guardalben E, Bergamini C, Cavalieri E, Fato R et al (2012) α-bisabolol is an effective proapoptotic agent against BCR-ABL(+) cells in synergism with Imatinib and Nilotinib. PLoS One 7:e46674
3. Bonifacio M, Rigo A, Bonalumi A, Guardalben E, Nichele I, Sissa C et al (2011) The sesquiterpene oil α-bisabolol induces apoptosis of B-chronic lymphocytic leukemia primary cells. Blood (ASH Annual Meeting Abstracts) 118:1319
4. Seki T, Kokuryo T, Yokoyama Y, Suzuki H, Itatsu K, Nakagawa A et al (2011) Antitumor effect of α-bisabolol against pancreatic cancer. Cancer Sci 102:2199–2205
5. Costarelli L, Malavolta M, Giacconi R, Cipriano C, Gasparini N, Tesei S et al (2010) In vivo effect of α-bisabolol, a non toxic sesquiterpene alcohol, on the induction of spontaneous mammary tumors in HER-2/neu transgenic mice. Oncol Res 18:409–418
6. Cavalieri E, Mariotto S, Fabrizi C, de Prati AC, Gottardo R, Leone S et al (2004) α-Bisabolol, a nontoxic natural compound, strongly induces apoptosis in glioma cells. Biochem Biophys Res Commun 315:589–594
7. Cavalieri E, Bergamini C, Mariotto S, Leoni S, Perbellini L, Darra E et al (2009) Involvement of mitochondrial permeability transition pore opening in α-bisabolol induced apoptosis. FEBS J 276:3990–4000
8. Chen W, Hou J, Yin Y, Jang J, Zheng Z, Fan H, Zou G (2010) α-Bisabolol induces dose- and time-dependent apoptosis in HepG2 cells via a Fas- and mitochondrial-related pathway, involves p53 and NFkappaB. Biochem Pharmacol 80:247–254
9. Darra E, Abdel-Azeim S, Manara A, Shoji K, Maréchal JD, Mariotto S et al (2008) Insight into the apoptosis-inducing action of α-bisabolol towards malignant tumor cells: involvement of lipid rafts and Bid. Arch Biochem Biophys 476:113–123
10. Maiuri MC, Zalckvar E, Kimchi A, Kroemer G (2007) Self-eating and self-killing: crosstalk between autophagy and apoptosis. Nat Rev Mol Cell Biol 8:741–752
11. Mariño G, Niso-Santano M, Baehrecke EH, Kroemer G (2014) Self-consumption: the interplay of autophagy and apoptosis. Nat Rev Mol Cell Biol 15:81–94
12. Nishida Y, Arakawa S, Fujitani K, Yamaguchi H, Mizuta T, Kanaseki T et al (2009) Discovery of Atg5/Atg7-independent alternative macroautophagy. Nature 461:654–658
13. Deretic V, Saitoh T, Akira S (2013) Autophagy in infection, inflammation and immunity. Nat Rev Immunol 13:722–737
14. Vicencio JM, Galluzzi L, Tajeddine N, Ortiz C, Criollo A, Tasdemir E et al (2008) Senescence, apoptosis or autophagy? When a damaged cell must decide its path, a mini-review. Gerontology 54:92–99
15. Kroemer G, Levine B (2008) Autophagic cell death: the story of a misnomer. Nat Rev Mol Cell Biol 9:1004–1010
16. Chipuk JE, Moldoveanu T, Llambi F, Parsons MJ, Green DR (2010) The BCL-2 family reunion. Mol Cell 37:299–310
17. Maiuri MC, Criollo A, Tasdemir E, Vicencio JM, Tajeddine N, Hickman JA et al (2007) BH3-only proteins and BH3 mimetics induce autophagy by competitively disrupting the interaction between Beclin 1 and Bcl-2/Bcl-X(L). Autophagy 3:374–376
18. Malik SA, Orhon I, Morselli E, Criollo A, Shen S, Mariño G et al (2011) BH3 mimetics activate multiple pro-autophagic pathways. Oncogene 30:3918–3929
19. Maiuri MC, Criollo A, Kroemer G (2010) Crosstalk between apoptosis and autophagy within the Beclin 1 interactome. EMBO J 29:515–516
20. Eskes R, Desagher S, Antonsson B, Martinou JC (2000) Bid induces the oligomerization and insertion of Bax into the outer mitochondrial membrane. Mol Cell Biol 20:929–935
21. Kroemer G, Jaattela M (2005) Lysosomes and autophagy in cell death control. Nat Rev Cancer 5:886–897
22. Klayman DL (1985) Qinghaosu (artemisinin): an antimalarial drug from China. Science 228:1049–1055
23. Wang X, Zhang C, Yan X, Lan B, Wang J, Wei C et al (2015) A novel bioavailable BH3 mimetic efficiently inhibits colon cancer via cascade effects of mitochondria. Clin Cancer Res 22(6): 1445–1458
24. Vinante F, Rigo A, Vincenzi C, Ricetti MM, Marrocchella R, Chilosi M et al (1993) IL-8 mRNA expression and IL-8 production by acute myeloid leukemia cells. Leukemia 7:1552–1556
25. Vinante F, Rigo A, Tecchio C, Morosato L, Nadali G, Chilosi M et al (1998) Serum levels of p55 and p75 soluble TNF receptors in adult acute leukaemia at diagnosis: correlation with clinical

and biological features and outcome. Br J Haematol 102: 1025–1034
26. Vinante F, Rigo A, Papini E, Cassatella MA, Pizzolo G (1999) Heparin-binding epidermal growth factor-like growth factor/diphtheria toxin receptor expression by acute myeloid leukemia cells. Blood 93:1715–1723
27. Rigo A, Gottardi M, Zamò A, Mauri P, Bonifacio M, Krampera M et al (2010) Macrophages may promote cancer growth via a GM-CSF/HB-EGF paracrine loop that is enhanced by CXCL12. Mol Cancer 9:273
28. van Nierop K, Muller FJ, Stap J, Van Noorden CJ, van Eijk M, de Groot C (2006) Lysosomal destabilization contributes to apoptosis of germinal center B-lymphocytes. J Histochem Cytochem 54:1425–1435
29. Guicciardi ME, Leist M, Gores GJ (2004) Lysosomes in cell death. Oncogene 23:2881–2890
30. Vinante F, Marchi M, Rigo A, Scapini P, Pizzolo G, Cassatella MA (1999) Granulocyte-macrophage colony-stimulating factor induces expression of heparin-binding epidermal growth factor-like growth factor/diphtheria toxin receptor and sensitivity to diphtheria toxin in human neutrophils. Blood 94:3169–3177
31. Vinante F, Rigo A (2013) Heparin-binding epidermal growth factor-like growth factor/diphtheria toxin receptor in normal and neoplastic hematopoiesis. Toxins (Basel) 5:1180–1201
32. Schweers RL, Zhang J, Randall MS, Loyd MR, Li W, Dorsey FC et al (2007) NIX is required for programmed mitochondrial clearance during reticulocyte maturation. Proc Natl Acad Sci USA 104:19500–19505
33. Rothe K, Lin H, Lin KB, Leung A, Wang HM, Malekesmaeili M et al (2014) The core autophagy protein ATG4B is a potential biomarker and therapeutic target in CML stem/progenitor cells. Blood 123:3622–3634
34. Vinante F, Rigo A, Scupoli MT, Pizzolo G (2002) CD30 triggering by agonistic antibodies regulates CXCR4 expression and CXCL12 chemotactic activity in the cell line L540. Blood 99:52–60
35. Rodríguez-Enfedaque A, Delmas E, Guillaume A, Gaumer S, Mignotte B, Vayssiére JL, Renaud F (2012) zVAD-fmk upregulates caspase-9 cleavage and activity in etoposide-induced cell death of mouse embryonic fibroblasts. Biochem Biophys Acta 1823:1343–1352
36. Rigo A, Gottardi M, Damiani E, Bonifacio M, Ferrarini I, Mauri P, Vinante F (2012) CXCL12 and [N33A]CXCL12 in 5637 and HeLa cells: regulating HER1 phosphorylation via calmodulin/calcineurin. PLoS One 7:e34432
37. Quah BJ, Warren HS, Parish CR (2007) Monitoring lymphocyte proliferation in vitro and in vivo with the intracellular fluorescent dye carboxyfluorescein diacetate succinimidyl ester. Nat Protoc 2:2049–2056
38. Troiano L, Ferraresi R, Lugli E, Nemes E, Roat E, Nasi M et al (2007) Multiparametric analysis of cells with different mitochondrial membrane potential during apoptosis by polychromatic flow cytometry. Nat Protoc 2:2719–2727
39. Galluzzi L, Zamzami N, de La Motte Rouge T, Lemaire C, Brenner C, Kroemer G (2007) Methods for the assessment of mitochondrial membrane permeabilization in apoptosis. Apoptosis 12:803–813
40. Métivier D, Dallaporta B, Zamzami N, Larochette N, Susin SA, Marzo I, Kroemer G (1998) Cytofluorometric detection of mitochondrial alterations in early CD95/Fas/APO-1-triggered apoptosis of Jurkat T lymphoma cells. Comparison of seven mitochondrion-specific fluorochromes. Immunol Lett 61:157–163
41. Bradley DF, Wolf MK (1959) Aggregation of dyes bound to polyanions. Proc Natl Acad Sci USA 145:944–952
42. Olsson GM, Rungby J, Rundquist I, Brunk UT (1989) Evaluation of lysosomal stability in living cultured macrophages by cytofuorometry. Effect of silver lactate and hypotonic conditions. Virchows Arch B Cell Pathol Mol Pathol 56:263–269
43. Zdolsek JM, Olsson GM, Brunk UT (1990) Photooxidative damage to lysosomes of cultured macrophages by acridine orange. Photochem Photobiol 51:67–76
44. Servais H, Van Der Smissen P, Thirion G, Van Der Essen G, Van Bambeke F, Tulkens PM, Mingeot-Leclercq MP (2005) Gentamicin-induced apoptosis in LLC-PK1 cells: involvement of lysosomes and mitochondria. Toxicol Appl Pharmacol 206: 321–333
45. Zareba M, Raciti MW, Henry MM, Sarna T, Burke JM (2006) Oxidative stress in ARPE-19 cultures: do melanosomes confer cytoprotection? Free Radic Biol 40(1):87–100
46. Yoon J, Kim KJ, Choi YW, Shin HS, Kim YH, Min J (2010) The dependence of enhanced lysosomal activity on the cellular aging of bovine aortic endothelial cells. Mol Cell Biochem 340: 175–178
47. Arsham AM, Neufeld TP (2009) A genetic screen in Drosophila reveals novel cytoprotective functions of the autophagy-lysosome pathway. PLoS One 4:e6068
48. Xia T, Kovochich M, Liong M, Zink JI, Nel AE (2008) Cationic polystyrene nanosphere toxicity depends on cell-specific endocytic and mitochondrial injury pathways. ACS Nano 2:85–96
49. Settembre C, Fraldi A, Medina DL, Ballabio A (2013) Signals from the lysosome: a control centre for cellular clearance and energy metabolism. Nat Rev Mol Cell Biol 14:283–296
50. Mizushima N, Levine B, Cuervo AM, Klionsky DJ (2008) Autophagy fights disease through cellular self-digestion. Nature 451:1069–1075
51. Guicciardi ME, Bronk SF, Werneburg NW, Yin XM, Gores GJ (2005) Bid is upstream of lysosome-mediated caspase 2 activation in tumor necrosis factor alpha-induced hepatocyte apoptosis. Gastroenterology 129:269–284
52. Billen LP, Shamas-Din A, Andrews DW (2009) Bid: a Bax-like BH3 protein. Oncogene 27(Suppl 1):93–104
53. Michaud M, Martins I, Sukkurwala AQ, Adjemian S, Ma Y, Pellegatti P et al (2011) Autophagy-dependent anticancer immune responses induced by chemotherapeutic agents in mice. Science 334:1573–1577
54. Howitz KT, Sinclair DA (2008) Xenohormesis: sensing the chemical cues of other species. Cell 133:387–391
55. Inoue Y, Shiraishi A, Hada T, Hirose K, Hamashima H, Shimada J (2004) The antibacterial effects of terpene alcohols on *Staphylococcus aureus* and their mode of action. FEMS Microbiol Lett 237:325–331
56. Teh OK, Hofius D (2014) Membrane trafficking and autophagy in pathogen-triggered cell death and immunity. J Exp Bot 65: 1297–1312
57. Kabbage M, Williams B, Dickman MB (2013) Cell death control: the interplay of apoptosis and autophagy in the pathogenicity of *Sclerotinia sclerotiorum*. PLoS Pathog 9:e1003287
58. Abramovitch RB, Kim Y-J, Chen S, Dickman MB, Martin GB (2003) Pseudomonas type III effector AvrPtoB induces plant disease susceptibility by inhibition of host programmed cell death. EMBO J 22:60–69
59. De Vleesschauwer D, Gheysen G, Höfte M (2013) Hormone defense networking in rice: tales from a different world. Trends Plant Sci 18:555–565
60. Pieterse CM, Leon-Reyes A, Van der Ent S, Van Wees SC (2009) Networking by small-molecule hormones in plant immunity. Nat Chem Biol 5:308–316
61. Jones JDG, Dangl JL (2006) The plant immune system. Nature 444:323–329
62. Dangl JL, Horvath DM, Staskawicz BJ (2013) Pivoting the plant immune system from dissection to deployment. Science 341:746–751